Clim. Past Discuss., 8, 6269–6308, 2012
www.clim-past-discuss.net/8/6269/2012/
doi:10.5194/cpd-8-6269-2012

Climate of the Past Discussions

Glacial fluctuations of the Indian monsoon and their relationship with North Atlantic abrupt climate change: new data and climate experiments

C. Marzin[1,*], N. Kallel[2], M. Kageyama[1], J.-C. Duplessy[1], and P. Braconnot[1]

[1]Laboratoire des Sciences du Climat et de l'Environnement/IPSL, CEA-CNRS-UVSQ – UMR8212, CE Saclay, l'Orme des Merisiers, 91191 Gif-sur-Yvette Cedex, France
[2]Université de Sfax, Faculté des Sciences, Laboratoire GEOGLOB, BP 802, 3038 Sfax, Tunisia
[*]now at: Met Office, Exeter, UK

Received: 31 July 2012 – Accepted: 16 August 2012 – Published: 18 December 2012

Correspondence to: C. Marzin (charline.marzin@metoffice.gov.uk)

Published by Copernicus Publications on behalf of the European Geosciences Union.

Abstract

Several paleoclimate records such as Chinese loess and speleothem sequences or upwelling indicators present large variations of the Asian monsoon system during the last glaciation. Here, a unique record in the northern Andaman Sea (core MD77-176) is used to reconstruct the variations of the hydrological cycle of the Bay of Bengal. The high resolution salinity record displays large millennial scale oscillations over the period 40 000 to 11 000 yr BP that are synchronous with the Greenland ice core record of changes in polar air temperature during the last glaciations. Events of high (resp. low) salinity in the Bay of Bengal, i.e. weak (resp. strong) Indian monsoon, correspond to cold (resp. warm) events in the North Atlantic. We use the IPSL_CM4 model to study the processes that can explain the relationship between the Indian monsoon and the North Atlantic climate. A modelling experiment represents such a rapid event in the North Atlantic under glacial conditions by increasing the freshwater flux in the North Atlantic and reducing the intensity of the Atlantic meridional overturning circulation. This freshwater hosing results in a weakening of the Indian monsoon rainfall and circulation. The changes in the continental runoff and local hydrological cycle are responsible for the changes in salinity of the Bay of Bengal in the model. This is a favourable comparison with the new salinity record presented here. Additional sensitivity experiments are produced with the LMDZ atmospheric model to analyse the teleconnection mechanisms between the North Atlantic and the Indian monsoon. The changes over the tropical Atlantic are shown to be essential in triggering perturbations of the subtropical jet over Eurasia that in turn affect the intensity of the Indian monsoon.

1 Introduction

During the last glaciation, the presence of large ice sheets and reduced atmospheric CO_2 concentration resulted in a drier climate and weaker monsoon systems over Asia as observed in several paleorecords. Modelling experiments from have shown that a reduction in moisture transport resulted in less precipitation over East Asia at the Last Glacial Maximum (LGM). The Paleoclimate Modeling Intercomparison Project 2 (PMIP2) indicates that the Indian monsoon rainfall was reduced in all models in the LGM experiments (up to 1.7 mm day^{-1}, Braconnot et al., 2007) due to prescribed LGM ice sheets and atmospheric CO_2 concentration conditions (differences in orbital forcing are small).

However, conditions prevailing during the LGM are not representative of the whole glaciation. The climate of the last glaciation was characterized by rapid climate changes in the North Atlantic/Greenland region associated to the Heinrich and Dansgaard/Oeschger (D/O) events (Heinrich, 1988; Bond et al., 1992; Broecker et al., 1992; Dansgaard et al., 1993; Grootes et al., 1993; Meese et al., 1997). Correlative climate changes have been identified in high resolution climate records from areas as distant as Santa Barbara Basin (Behl and Kennett, 1996), western and southern Europe (Thouveny et al., 1994; Allen et al., 1999), Socotra Island in the Arabian Sea (Burns et al., 2003), China (Wang et al., 2001) and Antarctica (EPICA Community Members, 2006). The abrupt changes in the North Atlantic climate have been associated with changes in the Atlantic meridional overturning circulation (AMOC) (McManus et al., 1999; Elliot et al., 2002; McManus et al., 2004; Stocker and Johnsen, 2003). The Asian monsoon, which depends on orbitally-controlled changes of insolation (Xiao et al., 1999; Rousseau and Kukla, 2000) also varied on millennial timescales as in speleothem (Wang et al., 2001) and denitrification records (Altabet et al., 2002). However, the intensity of the corresponding variations in the hydrological cycle, a major aspect of the Indian monsoon, has not been documented. The Bay of Bengal, which receives the outflow of the major rivers draining the Himalayan mountains and the Indian subcontinent, is very sensitive to changes in the hydrological cycle and continental runoff in South Asia (Prell et al., 1980; Duplessy, 1982). Here, we have measured surface water oxygen isotope composition and reconstructed salinity variations recorded in a core raised from the southwest sector of the low surface salinity tongue of the northern Andaman Sea, an area which today directly receives the discharge of the Irrawady

CPD
8, 6269–6308, 2012

and Salween rivers. We show that, as for previous records of millennial changes of the glacial Asian monsoon, the Indian monsoon fluctuates simultaneously with the abrupt climate changes recorded in the North Atlantic.

Understanding this teleconnection between the North Atlantic/Arctic climate and the Indian monsoon intensity is a challenge both for future and past climate changes (Khare, 2008). More generally, the tropical/extratropical teleconnection related to the abrupt climate changes of the last glacial period are not well understood, as underlined by the review Clement and Peterson (2008). The teleconnection mechanisms explaining the correlative rapid climate variations between the North Atlantic and the Indian monsoon region in the past have been investigated through modelling experiments mostly under present day climate conditions (Vellinga and Wood, 2002; Zhang and Delworth, 2005; Lu and Dong, 2008). Zhang and Delworth (2005) analyzed the tropical response to a weakened AMOC and suggested that the Indian monsoon is weakened due to a weakening of the Walker circulation in the southern tropical Pacific. Lu and Dong (2008) found that the atmospheric teleconnection in the eastern and central North Pacific and the atmosphere-ocean interaction in the tropical North Pacific play the most important role. Using a model of intermediate complexity, Jin et al. (2007) also suggest that the Asian monsoon circulation is weakened during Heinrich events of the last glacial age. In addition, several studies have analyzed the relationship between a warm phase of the North Atlantic Multidecadal Oscillation (AMO) and a strong Indian monsoon (Zhang and Delworth, 2006; Goswami et al., 2006; Lu et al., 2006; Li and Harrison, 2008; Feng and Hu, 2008). Using observations, Goswami et al. (2006) and Feng and Hu (2008) propose a link between the North Atlantic surface temperature and the Indian monsoon intensity through a physical mechanism affecting the meridional gradient of upper tropospheric temperature between the Tibetan Plateau and the tropical Indian Ocean. This meridional gradient of temperature has been shown to be an indicator of the timing and intensity of the summer monsoon season (He et al., 2003; Goswami and Xavier, 2005).

CPD
8, 6269–6308, 2012

Modelling experiments usually represent abrupt glacial climate changes as responses to fluctuations of the AMOC triggered by freshwater discharges in the North Atlantic as reviewed in Clement and Peterson (2008) and Kageyama et al. (2010). Several general circulation models have now been used for such glacial freshwater hosing experiments and obtain a reduction of the Indian monsoon when the AMOC weakens (Kageyama et al., 2009; Merkel et al., 2010; Otto-Bliesner and Brady, 2010). Using the IPSL-CM4 ocean-atmosphere coupled model, we have shown that a collapse of the AMOC under glacial conditions also leads to a significant weakening of the Indian monsoon (Kageyama et al., 2009). This weakening appears to be related to the upper tropospheric cooling to the North of the Indian subcontinent, that is occurring simultaneously with the AMOC weakening. Following our previous study, we focus here on an analysis of the impact of an AMOC collapse on the Indian monsoon and on the hydrological cycle of the Bay of Bengal in our original coupled experiment. It is difficult to discern the teleconnection mechanisms between the North Atlantic and the Indian monsoon region from these coupled experiments alone because the weakening of the AMOC affects sea surface temperatures (SST) over all oceans, including the North and the tropical Atlantic that are both key regions for the Indian monsoon. We therefore performed additional sensitivity experiments in order to investigate which region of SST changes has the strongest impact on monsoon changes and what are the mechanisms for this North Atlantic/Indian monsoon teleconnection. We then investigate if the relationship we find between tropical SST changes and those in Indian monsoon precipitation holds in additional coupled model experiments in which we force the AMOC to recover.

Section 2 discusses the method and the results of the North Andaman Sea record for the last 40 000 yr. The expriment in which we simulate the AMOC collapse and its impact on the Indian monsoon is presented in Sect. 3, as well as the additional sensitivity experiments. In Sect. 3.4 we present the results from the additional coupled experiments in which the AMOC resumes. The study is discussed and concluded in Sect. 4.

CPD
8, 6269–6308, 2012

2 Indian monsoon variability in the 40 000 yr record in the Bay of Bengal

2.1 Material and methods

Core MD77-176 (14°31′ N; 93°08′ E; 1375 m water depth) has been selected to estimate surface salinity variations in the Bay of Bengal (Fig. 1). This core, which is located in the southwest sector of the present low surface salinity tongue of the northern Andaman Sea, also records the extreme dryness of the LGM Asian monsoon climate (Duplessy, 1982) and should be very sensitive to fluctuations of the hydrological cycle and continental runoff in the Irrawady-Salween drainage basin.

Oxygen isotope measurements ($\delta^{18}O$) were made on planktonic foraminifera Globigerinoides ruber (Fig. 2). The $\delta^{18}O$ values of planktonic foraminifera record changes in both the oxygen isotope composition of sea surface water δ_w and the isotopic fractionation between calcium carbonate and water, which depends upon the temperature at which foraminifera have formed their shell (Epstein et al., 1953; Shackleton, 1974).

In core MD77-176, sea surface temperature (SST) estimates were derived from foraminiferal counts, using the modern analogue technique (Hutson, 1979; Prentice, 1980; Overpeck et al., 1985). The squared chord distance dissimilarity coefficient was used to measure the mean degree of dissimilarity between each fossil assemblage and the modern analogues. It never exceeds 0.16 and the ten best modern analogues were selected to estimates past SST with a statistical error smaller than 1 °C at 1σ (Fig. 2).

The SST record exhibits no significant changes from the glacial period to the Holocene (Fig. 2). These results are consistent with all SSTs reconstructed using planktonic foraminiferal assemblages for this region (Cullen, 1981; Barrows and Juggins, 2005), but contrast with the 2 to 3 °C cooling inferred from Mg/Ca and Uk-37 SST data in the same area (Rashid et al., 2007; Kudrass et al., 2001). In all cases, the SST changes from the glacial to interglacial conditions are too small to explain the recorded $\delta^{18}O$ variations. The foraminiferal $\delta^{18}O$ record can thus be considered as a good approximation of the changes in the oxygen isotope composition of the surface water at the location of our core.

CPD
8, 6269–6308, 2012

Sea water δ^{18}O variations directly reflect those of surface water δ^{18}O due to both global ice volume changes (Emiliani, 1954) and local freshwater budget (Precipitation + Runoff – Evaporation) variations (Craig and Gordon, 1965; Delaygue et al., 2001). In order to subtract the global ice volume record (Waelbroeck et al., 2002) from the δ^{18}O record, we generated an absolute chronology using AMS radio-carbon dating on monospecific planktonic foraminiferal samples. For the last 20 ky, ^{14}C ages have been converted into calendar ages using the Calib 4.1 program (Stuiver and Reimer, 1993; Stuiver et al., 1998), which includes the correction for the ocean surface reservoir age (Broecker and Peng, 1982). This correction was assumed to be constant and equal to 400 yr because air-sea exchanges have always been high in tropical waters. The conversion of ^{14}C ages to calendar ages is less accurate before 20 ky ^{14}C BP, because the ^{14}C production rates in the upper atmosphere experienced major changes during the last glaciation (Laj et al., 1996; Voelker et al., 1998; Bard, 1998; Hughen et al., 2004; van der Plicht et al., 2004; Fairbanks et al., 2005) and different calibration models provide age estimates, which can differ by more than 2 ky.

The high resolution local δ_w record of core MD77-176 displays large millennial scale oscillations over the period 40 000 to 11 000 yr BP (Fig. 3). They closely correlate to the Greenland ice core record of changes in polar air temperature during the last glaciation. This correlation is in good agreement with previous observations of enhanced summer monsoon activity during D/O events (Wang et al., 2001; Burns et al., 2003). We have therefore developed a second age model for core MD77-176 assuming that local δ_w changes in the Northern Andaman Sea and GISP2 δ^{18}O are in phase and synchronous. Comparison of this new age model with the ages calibrated using the Fairbanks et al. (2005) model before 20 ^{14}C ky BP indicates that our assumption is realistic (Fig. 3). Between 13 and 10.5 ky BP, Fig. 3a displays a difference of about 1 to 1.5 ky between the age model based on calibrated ^{14}C ages and that obtained by correlation with GISP2 δ^{18}O record. During Younger Dryas for instance, the calibrated ^{14}C ages of the lowering of the Bay of Bengal δ_w is older than the cooling of the North Atlantic Younger Dryas by 1 to 1.5 kyr. This age anomaly is a local phenomenon as it is not observed in other cores, which are protected from the direct influence of rivers outflow (Rashid et al., 2007).

2.2 Results

Core MD77-176 faithfully records the enhanced southwest monsoon rains over the Indian subcontinent at the beginning of the Holocene (Fontes et al., 1996; Gasse et al., 1996; VanCampo et al., 1996; COHMAP Members, 1988; VanCampo and Gasse, 1993). During the lower Holocene to about 4 ky BP, the surface water δ^{18}O (δ_w) was lower than today by about 0.2 to 0.8 ‰ in the Bay of Bengal. Considering the δ_w/salinity slope in the Northern Indian Ocean (0.25 to 0.37 ‰; Delaygue et al., 2001; Rostek et al., 1993), the corresponding surface salinity decrease is of about 0.5 to 2.5 ‰ (Fig. 3b).

During the glaciation, the local sea water δ^{18}O record of core MD77-176 displays many periods during which the freshwater input exhibits significant variations (Fig. 3b). The highest surface salinities were reached during the Last Glacial Maximum. From 40 to 28 ky BP, surface salinity values were lower than those of the LGM but higher than today. These observations are in agreement with the loess deposits records in southern and southeastern Tibet and in western China (Porter and An, 1995; Xiao et al., 1995; Guo et al., 1996; Chen et al., 1997; An et al., 1991, 1993) and with the changes in the intensity of Somalian and Arabian upwelling (Sirocko et al., 1991; Zonneveld et al., 1997), which show that the Indian summer monsoon was generally weak during the glaciation and always weaker than today.

The general trend described above is complicated by large abrupt changes of millennial scale. During the LGM, three episodes of low surface salinity were centered at about 23, 20.5 and 19 ky BP (Fig. 3b). Also, during the upper part of the Marine Isotope Stage 3, 5 events of salinity decrease are recorded in core MD77-176. They occurred at about 37.5, 35, 33.5, 32 and 27 ky BP. All these low salinity episodes observed in the Andaman Sea have equivalent warm episodes in the Greenland ice

CPD
8, 6269–6308, 2012

record (interstadials). During these events, summer monsoon was thus stronger than today and it resulted in significant rainfall over the Indian subcontinent.

Between the freshwater injection events into the Bay of Bengal, events of salinity increase reflecting extreme monsoon weakness are recorded. Four of them have been detected in Chinese loess sequences (at around 39, 31, 24 and 16 ky BP), and are characterized by lower continental weathering intensity and coarser grain size peaks in the loess records (Porter and An, 1995; Xiao et al., 1995; Guo et al., 1996; Chen et al., 1997). Like the high salinity events in the Bay of Bengal, the Chinese dry/cold episodes are found to be synchronous with the last four North Atlantic Heinrich events. However, not all the periods of marked reduction in the continental runoff into the Bay of Bengal during the last 40 000 yr correlate with Heinrich events and some cold stadials of the Greenland ice records are also correlated with extremely dry conditions over Asia.

The record of core MD77-176 displays a remarkable similarity with the oxygen isotope records of eastern China stalagmites (Wang et al., 2001; Cosford et al., 2008) and the nitrogen isotope ratio variations recorded in Arabian Sea sediment (Altabet et al., 2002). These records are also directly linked to the monsoon intensity. Eastern China stalagmites δ^{18}O values are controlled by the summer/winter precipitation ratio. Summer precipitation δ^{18}O is about 10 ‰ lower than that of winter. Warmer Greenland temperatures were found to correlate with periods of more intense summer East Asian Monsoon and therefore with more contribution of summer precipitation. In the Arabian Sea, δ^{15}N and thus denitrification were found to be high during the warm phases of the Dansgaard/Oeschger events and low during the cold phases of these events. High δ^{15}N values are interpreted as an indication of higher primary productivity and higher denitrification in the Arabian Sea which are largely the result more active upwelling and thus stronger summer monsoon winds (Altabet et al., 2002).

Therefore, warming in the North Atlantic area coincides with active glacial Indian summer monsoon circulation. Even within the last glacial maximum, which was not the coldest glacial period in the middle latitudes North Atlantic records (Duplessy et al., 1991), some short events of active summer monsoon circulation occurred in southeastern Asia. A similar relative strengthening of the Indian monsoon during the LGM was also inferred from the Somali and Arabian Sea upwelling records (Zonneveld et al., 1997; Sirocko et al., 1991). Nevertheless, our data demonstrate that the periods of Indian summer monsoon intensification during the last glaciation were not characterized by precipitation as intense as those of Holocene. Our data show that the hydrological cycle associated with the monsoon is highly sensitive and responds rapidly to abrupt climatic variations over the North Atlantic area.

While glacial vs. Holocene vs. present monsoon fluctuations have been analysed via numerical experiments, the teleconnection with the North Atlantic abrupt events in glacial times has not been extensively studied. We therefore focus on this aspect with the following analysis.

3 Modelling study of the Indian monsoon response to a freshwater hosing under glacial conditions

3.1 Model and experiments

In order to better understand the mechanisms relating the rapid variations of monsoon activity seen in the paleo-record presented above and those recorded in the North Atlantic and Greenland area, we analyse two modelling experiments to evaluate the impact of a freshwater hosing experiment on the Indian monsoon under glacial conditions. The model used in the present study is the coupled ocean-atmosphere IPSL-CM4 model (Marti et al., 2010). The atmospheric component of this coupled model is LMDZ.3.3 (Hourdin et al., 2006), with resolution 96 × 71 × 19 in longitude × latitude × altitude. The horizontal grid is regular, while the vertical levels are more numerous near the surface. This atmospheric component is coupled with the land surface scheme ORCHIDEE (Krinner et al., 2005) which includes a river routing scheme for the 50 largest river basins in order to close the water budget between land and ocean (Ngo-Duc et al., 2005). The ocean component is ORCA2 (Madec et al., 1998), which uses an irregular horizontal grid of 182 × 149 points with a resolution of 2°, refined over key regions such as the North Atlantic and near the Equator. This model has 31 depth levels. The sea-ice component is the Louvain-la-Neuve Ice Model (LIM2, Fichefet and Maqueda, 1997). The coupling of these components is performed using the OASIS (version 3) coupler (Valcke, 2006).

The glacial conditions are obtained by first simulating the Last Glacial Maximum (LGM) climate following the PMIP2 (Paleo-Modelling Intercomparison Project phase 2, Braconnot et al., 2007, http://pmip2.lsce.ipsl.fr/) protocol: we use the ICE-5G ice-sheet reconstruction (Peltier, 2004), atmospheric gas concentrations (Monnin et al., 2001; Dallenbach et al., 2000; Flückiger et al., 1999) and orbital parameters (Berger, 1978) for 21 ky BP. The river pathways are adapted for the LGM (Alkama et al., 2007). The control experiment is labeled LGMc (c for control) and presents an active AMOC (maximum overturning in the North Atlantic of 18 Sv). The second simulation is a hosing experiment obtained by adding a 0.18 Sv freshwater input in the North Atlantic, resulting in a collapse of the AMOC (which reaches 2 Sv after 250 yr) and is labeled LGMh (h for hosing). This latter experiment is therefore a highly idealized simulation of a Heinrich event under glacial conditions. The climatologies presented in this study are integrated over the years 201–250 for LGMc and 371–420 for LGMh. More details on the experimental set up and on the AMOC response to the freshwater input can be found in Kageyama et al. (2009), in which LGMc is labelled “LGMa” and LGMh is labelled “LGMc”.

The evaluation of the IPSL-CM4 coupled model is presented in Marti et al. (2010). In present day conditions, the model performs well in the tropical area. There is an underestimation of the amount of Indian monsoon rainfall over the land but the monsoon circulation is well depicted over the Indian Ocean. The model results for the Mid-Holocene compare well with other models from the PMIP2 project (Braconnot et al., 2007). Using the same model, Marzin and Braconnot (2009) have shown that the Indian monsoon is sensitive to the precession changes between the Early Holocene, the Mid-Holocene and the preindustrial periods. These results indicate a gradual weakening of the Indian

CPD
8, 6269–6308, 2012

monsoon intensity throughout the Holocene and are consistent with the surface salinity evolution at the MD-77176 core site and with other paleo-records of monsoon intensity. Regarding the LGM experiment, the Indian monsoon is not very sensitive to the LGM conditions compared to other PMIP2 models (Braconnot et al., 2007). This could be due to the fact that the AMOC is strong in this LGM control simulation and therefore it would correspond to a "warm" phase of a D/O event, with a monsoon not very different from today (Braconnot et al., 2007), and that the Indian monsoon is already weak in the control simulation. However, the hosing experiment presents a much weaker AMOC and can be considered as representative of a Heinrich event.

Finally, we test our mechanism for the relationship between the AMOC state and the Indian monsoon by using additional ISPL_CM4 coupled experiments run under the same LGM boundary conditions. The first experiment is the continuation of LGMh but with no fresh water hosing applied. In this simulation (in dark blue and labelled "LGM AMOC" off on Fig. 8) the AMOC never recovers. In the second experiment (in orange, labelled "–0.1 Sv") we have applied a negative fresh water flux in the North Atlantic between 50 and 70° N and as a result, the AMOC resumes after 350 yr to an AMOC of 18 Sv, i.e. equal to our reference state. This AMOC remains stable for another 70 yr, after which the simulation was stopped. The third set of experiments uses a stronger forcing of –0.5 Sv over the same region, from three initial states of the AMOC off simulation. In all these experiments (in red and labelled "–0.5 Sv") the AMOC resumes in less than 100 yr and reaches values larger than 20 Sv. These simulations were not run to equilibrium. We use all the years from these simulations to test our teleconnection mechanism in Sect. 3.4.

3.2 Indian monsoon weakening due to the collapse of the AMOC

All results are shown for the season averaged from June to September (JJAS) to encompass the whole boreal summer monsoon season (Fig. 4). The main features discussed are significant at the 95 % level based on a Student's t-test but the confidence intervals are not shown on the figures for more clarity. The freshwater input in the North

Atlantic/Arctic region and the collapse of the AMOC between LGMh and LGMc results in a dipolar pattern of SST anomalies in the Atlantic, with a more than 3°C cooling in the North Atlantic and a more than 1 °C warming in the South Atlantic (Fig. 4a). This typical cross-equatorial SST dipole is accompanied by a southward shift of the ITCZ in the Atlantic (Fig. 4b) that is consistent with previous studies (Stouffer et al., 2006; Timmermann et al., 2007; Wu and Kirtman, 2007; Chang et al., 2008). Significant remote impacts are also seen across the globe. The cooling of the North Atlantic extends across the whole Eurasian continent and the subtropical North-West Pacific, and a nearly overall warming of the Southern Ocean. The North Atlantic forcing leads to significant precipitation and circulation changes in the Pacific Ocean. These features are discussed in details in Kageyama et al. (2009) and are shown to be more pronounced in the case of the LGM than for other climatic periods (Swingedouw et al., 2009).

The North Atlantic hosing experiment results in a statistically significant reduction of the Indian monsoon precipitation to the north-east and south-west of the subcontinent by about 10 % (Fig. 4b). The reduction in precipitation coincides with the core regions of simulated monsoon precipitation. The monsoon cross-equatorial flow is weakened over the Indian Ocean, therefore reducing the moisture advection into the monsoon region. The strength of the southwesterly winds over the western Arabian Sea is reduced, which is consistent with paleo-records indicating changes in upwelling and productivity in this region coeval with North Atlantic changes (Schulz et al., 1998; Altabet et al., 2002; Gupta et al., 2003). The weakening of the Indian monsoon as a response to the freshwater input in the North Atlantic is consistent with other modelling studies discussed in the introduction, but our experiments confirm that this teleconnection holds under glacial conditions.

The reduction of the Indian monsoon intensity induces an increase in salinity over the whole Bay of Bengal (Fig. 4c). The amplitude of the anomalies are from 0.6 to 2 ‰ in the northern part of the Bay of Bengal, and are similar in amplitude to the large variations in the North Andaman Sea surface salinity record presented in Sect. 2.2. The fresh water content of the Bay of Bengal is under the influence of the fresh water input

Discussion Paper | Discussion Paper | Discussion Paper | Discussion Paper |

CPD
8, 6269–6308, 2012

Indian monsoon and North Atlantic abrupt climate change

C. Marzin et al.

(precipitation minus evaporation and continental river runoff), as well as water transport from the South. This is reflected in the large variations of mixed layer thickness across the Bay of Bengal during the summer months (Varkey et al., 1996). The freshwater input is diagnosed from the model outputs and our hosing experiment shows that the river runoff in the north coastal region of the Bay of Bengal drops by 20 % (by 0.02 to 0.06 × 10^{-3} kg m^{-2} s^{-1}) and the local freshwater input (precipitation minus evaporation) is also reduced over the whole Bay of Bengal by approximately 10 % (0.006 to 0.016 × 10^{-3} kg m^{-2} s^{-1}) due to suppressed local precipitation over the ocean (Fig. 4a). Therefore, the model results show that the changes in salinity over the Bay of Bengal highlighted in the Northern Andaman Sea record as well as in the model outputs, are sensitive to the suppression of the hydrological cycle both over the land (reduction in river runoff) and over the ocean (reduction in local precipitation). As a result, this modelling study supports the hypothesis used for the age model of the core MD77-176 assuming that the local changes of the Andaman Sea are synchronous with the abrupt events of the Greenland ice core records.

The large scale meridional gradient of upper tropospheric temperature (averaged from 200 to 500 hPa) over India has been shown to be an indicator of the monsoon seasonal evolution and intensity (He et al., 2003; Goswami and Xavier, 2005). This meridional gradient is considerably reduced in the hosing experiment (Fig. 4a) with the cooling anomaly over the Himalaya and is a direct indicator of the monsoon weakening. In our previous study (Kageyama et al., 2009), we have shown that the JJAS tropospheric temperature and the JJAS Indian monsoon rainfall are decreasing synchronously with the strength of the AMOC throughout the simulation. We have hypothesized that the predominant pathway from the North Atlantic perturbation to the Indian monsoon would be through the atmospheric circulation by affecting the large cooling of tropospheric temperature over the Eurasian continent.

The underlying mechanisms of this North Atlantic/Indian monsoon teleconnection are still being investigated by the community. In order to refine these analyses and to better understand the teleconnection mechanisms, we have performed sensitivity experiments presented in the following section. These are also designed to test some of the hypotheses presented in the introduction.

3.3 Sensitivity experiments and the dominant role of the tropical Atlantic

To differentiate the impact of SST changes of several key regions on the Indian monsoon, we have performed three sensitivity experiments using the atmospheric component of the coupled model. The SST fields from the coupled experiments were used to force the atmospheric model and we tested the impact of SST changes due to the freshwater forcing in specific regions. To do this, we applied the SSTs from the hosing experiment LGMh over the test region and the SSTs of the control experiment LGMc for the rest of the globe. In addition, to make sure that the atmospheric model replicates the results discussed above, we performed the atmosphere-only version of the control and the hosing experiments using the SSTs obtained from the coupled experiments over the whole globe (LGMcF and LGMhF). All the experiments are run for 50 yr and use SSTs from the last 50 yr of the previous subsection coupled simulations. The SST fields have monthly frequency so that the interannual variability of the coupled experiments is passed on to the forced experiments. The forced experiments performed are the following:

– LGMcF: simulation forced by the SST fields from the LGMc coupled control experiment over the whole globe.

– LGMhF: simulation forced by the SST fields from the LGMh coupled hosing experiment over the whole globe.

– LGMhNA: simulation forced by the SST fields from the LGMh simulation over the North Atlantic/Arctic region only (above 30° N), to analyze the impact of the North Atlantic cooling (Fig. 5b).

CPD
8, 6269–6308, 2012
Indian monsoon and North Atlantic abrupt climate change
C. Marzin et al.

– LGMhTA: simulation forced by the SST fields from the LGMh simulation over the tropical Atlantic region only (30° S to 30° N), to analyze the impact of the large dipolar SST anomaly (Fig. 5c).

– LGMhNTAC: complementary simulation of LGMhNA and LGMhTA forced by the SST fields from the LGMh simulation over all the oceans except the North Atlantic/Arctic and tropical Atlantic regions that are forced by SSTs from the LGMc control experiment, to analyze the impact of the SST changes over the Indian and Pacific Oceans (Fig. 5d).

The results of these sensitivity experiments are presented in terms of surface and upper tropospheric temperature change (Fig. 5), precipitation and low level circulation change (Fig. 6), and 200 hPa geopotentiel and circulation change (Fig. 7). The atmospheric model, forced by the SSTs from the previous coupled experiments, is able to reciprocate the precipitation results presented in Sect. 3.2 both in terms of precipitation change over the Indian region (Fig. 6a) and of upper tropospheric cooling over Eurasia (Fig. 5a). The first sensitivity experiment indicates that the North Atlantic cooling only has a marginal impact on precipitation over the Indian region (Fig. 6b). Hence, our results demonstrate that the North Atlantic cooling associated with the freshwater input alone is not sufficient to explain the monsoon weakening. Even though the cooling over Eurasia is significant, the upper tropospheric temperature (TT) is decreased by only 0.25 K over the Tibetan Plateau (Fig. 5b).

If only the SST perturbation over the tropical Atlantic is imposed (Fig. 5c), then the precipitation decrease seen in the coupled simulations over the south-west and north-east of India is fully recovered (Fig. 6c). The fact that the sole bipolar SST structure across the equatorial Atlantic is able to trigger such a response over the Indian region is remarkable. The TT signature over the Tibetan Plateau in this sensitivity experiment is larger than in LGMhNA, even though the decrease in surface temperatures does not extend as much over Eurasia (Fig. 5c). The weakening of the Indian monsoon intensity is associated with the reduction of the meridional gradient of upper

Discussion Paper | Discussion Paper | Discussion Paper | Discussion Paper |

CPD

8, 6269–6308, 2012

Indian monsoon and North Atlantic abrupt climate change

C. Marzin et al.

tropospheric temperature in a consistent way with previous studies (Goswami et al., 2006; Lu and Dong, 2008). However, these studies suggest that the North Atlantic temperature changes directly impact the Eurasian continent, but we show that in our case it is more directly influenced by the tropical Atlantic bipolar SST anomaly and the associated southward shift of the ITCZ.

In addition to this hypothesis of predominant link between the North Atlantic and the Indian monsoon through Eurasian continent, Zhang and Delworth (2005) and Lu and Dong (2008) suggest that the Indian monsoon is mostly influenced by changes in the tropical Pacific in their coupled experiments. Indeed, several studies show that the Atlantic perturbation is propagated to the Pacific through the Central American region (Dong and Sutton, 2002; Zhang and Delworth, 2005). Here, to isolate the impact of the Pacific Ocean and Indian Ocean SST changes in our modelling experiments, we have performed the complementary simulation LGMhNTAC. The cooling over the equatorial Pacific and the north eastern Pacific warming (Fig. 5d) are consistent with the above studies. The anticyclonic anomaly over the subtropical eastern Pacific enhances precipitation. A warming over the southern equatorial Indian Ocean is associated with an amplification of convective rainfall (Figs. 5d and 6d), and a large anomaly of reduced precipitation appears over the subtropical western Pacific. More strikingly, this sensitivity experiment shows that the SST changes in the Pacific and Indian Oceans actually amplify the monsoon rainfall over the south-west and the western part of the Bay of Bengal (Fig. 6d). This is associated with a positive anomaly of upper tropospheric temperature over the north-west of India. Indeed, it has been shown that the interannual variability of the Indian monsoon is very sensitive to the upper tropospheric warming over this region (Xavier et al., 2007).

Our sensitivity experiments show that the mechanisms that are suggested to be predominant in other studies are not sufficient to explain the impact of the AMOC weakening on the Indian monsoon rainfall. The North Atlantic SST changes cannot on their own directly produce a dampening of the monsoon activity. Moreover, the atmosphere and ocean interactions over the Pacific and Indian oceans actually result in

CPD
8, 6269–6308, 2012

an amplification of the Indian monsoon in our analysis. Therefore, using the sensitivity experiments, we isolate the impact of the tropical Atlantic SST changes associated with the large southward shift of the ITCZ as the predominant forcing. This bipolar SST anomaly is obtained both through atmospheric and oceanic pathways (Kageyama et al., 2009; Swingedouw et al., 2009), and we show with the atmosphere-only experiment LGMhTA that this anomaly is resulting in a weakening of the Indian monsoon through the Southern Eurasian continental cooling.

The tropical Atlantic SST anomaly induces perturbations of the stationary waves in the northern extratropics seen in the TT. The wavetrain perturbations are propagated downstream from the North Atlantic to Eurasia as seen from the negative anomalies of 200 hPa geopotential (Fig. 7c). The cyclonic anomalies of 200 hPa winds and the acceleration of the subtropical westerly jet stream obtained in LGMhF (Fig. 7a) are also fully represented in the LGMhTA simulation (Fig. 7c). This atmospheric teleconnection could be explained through the mechanism suggested by Ding and Wang (2005, 2007) who showed that the Indian monsoon is interacting with a circumglobal teleconnection pattern with specific centers of perturbation in the mid-latitudes. In our LGMhTA experiment, the largest TT anomaly over the north-west Atlantic is associated with another center of upper tropospheric cooling over the eastern Mediterranean region and over the Tibetan Plateau. Ding and Wang (2005) suggest that if a wave train is excited at the jet exit of the North Atlantic, this influences the central Asian high and the Indian monsoon. Kucharski et al. (2008) use observation datasets to analyze the Atlantic component of the Indian monsoon interannual variability and show that by subtracting the ENSO-forced component, the strong Indian monsoon years are correlated with the cold south equatorial Atlantic SSTs. Kucharski et al. (2009) and Losada et al. (2010) also highlight the teleconnection between the tropical Atlantic and the Indian monsoon circulation at shorther time scales. Therefore, the cold anomaly over the northern tropical Atlantic and the warm anomaly over the southern tropical Atlantic can both induce pathways to influence the reduction of the Indian monsoon circulation and precipitation.

Following the comment by Clement and Peterson (2008) that the contribution of the land surface snow cover and sensible heating over the Tibetan Plateau had not been investigated, we have verified that the Indian monsoon weakening is not driven by changes in the snow cover over the Tibetan Plateau as these are marginal in our experiments (not shown). The large scale deep upper tropospheric cooling over the Tibetan Plateau induced by the collapse of the AMOC is the main factor explaining the weakening of the Indian monsoon as suggested by Goswami et al. (2006). And we have shown that this is more effectively caused by the tropical Atlantic influence than by the North Atlantic cooling itself, the anomaly over the tropical Atlantic triggering a southward shift of the subtropical jet-stream, which acts to decrease the upper tropospheric temperatures over the key area of the Tibetan Plateau and finally the Indian Monsoon.

3.4 Testing the tropical teleconnection mechanisms in additional experiments in which the AMOC resumes

In this section, our objective is to test if the connection between the tropical SST changes and Indian monsoon precipitation is found in other coupled experiments in which the AMOC is forced to vary and if it is valid during the transitions between the different AMOC states which we have studied via our sensitivity experiments. We also want to examine if the pathway of the connection, via the upper-level subtropical jet-stream, is still valid.

Figure 8 shows results from all years of all the simulations (each year represented by a dot). The top left figure confirms the relationship between the intensity of the Indian monsoon and the strength of the Atlantic ocean northward transport: the lower the transport, the weaker the Indian monsoon. This relationship is broken down in different steps of the teleconnection pathway in the remaining three panels of this figure. On the top right panel, we use the 200 hPa zonal wind strength over the Sahara as a measure of the southward position of the subtropical jet-stream: the stronger the wind strength over this region, the more the subtropical jet-stream is located to the

CPD
8, 6269–6308, 2012

South over Africa. This panel shows that the stronger the jet-stream over the Sahara, the weaker the Indian monsoon. The lower left panel shows that this wind strength is larger for cooler North Atlantic SSTs (and for warmer South Atlantic SST, not shown). Finally, this North Atlantic SSTs are positively correlated with the Atlantic ocean transport. Thus, the pathway found thanks to our sensitivity experiments is confirmed by the extensive analysis of our coupled experiments in which the AMOC is forced to collapse and then to resume at different speeds. This shows that this pathway can act fast, even at interannual/decadal time-scales.

4 Conclusions

In this study, we attempt to give a new characterization of the Indian monsoon abrupt changes during the last glacial period by showing the results from a core from the North Andaman Sea and to understand those changes through dedicated modelling experiments. The Andaman Sea high resolution paleorecord shows very large salinity variations on the millenial scale in the Bay of Bengal that are interpreted as Indian monsoon fluctuations which have an impact on the hydrological cycle of the Bay of Bengal. Warming (resp. cooling) in the North Atlantic area and in the Greenland ice core record of changes in polar air temperature coincides with active (resp. weakened) glacial Indian summer monsoon circulation. Our data show that the hydrological cycle associated with the Indian monsoon is highly sensitive and responds rapidly to abrupt climatic variations over the North Atlantic area. Nevertheless, the periods of Indian summer monsoon intensification during the last glaciation were not characterized by precipitation as intense as those of the Holocene in this dataset.

A freshwater hosing numerical experiment under Last Glacial Maximum conditions is set up to test the interpretation of the paleorecord as Indian monsoon variations and to analyse the mechanisms of teleconnection between the North Atlantic abrupt events and the Bay of Bengal. In this simulation, the North Atlantic cools and the Indian monsoon rainfall and circulation weakens. The increase in salinity in the Bay of Bengal is due to a decrease in continental runoff and in local precipitation minus evaporation. The monsoon weakening is associated with an upper tropospheric temperature cooling over the Tibetan Plateau.

Sensitivity experiments to local SST changes are realised to test the teleconnection mechanism with the Indian monsoon, and a new teleconnection pathway is revealed. It is the dipole of SST anomalies obtained in the tropical Atlantic Ocean that impacts the most the Indian monsoon. These anomalies excite a wave train perturbation throughout the Eurasian continent with an associated acceleration of the subtropical westerly jet. The center of perturbation around the Tibetan Plateau directly affects the intensity of the monsoon through the reduction of the meridional tropospheric temperature gradient over India. We also show with these sensitivity tests that previously suggested mechanisms like the direct influence of the North Atlantic SST changes on the Indian monsoon and the ocean-atmosphere interactions in the Pacific are not sufficient to explain the changes obtained for the Indian monsoon in our model. Despite different previous freshwater hosing experiments showing different results in SST and precipitation over the Pacific and the Indian Ocean, the SST and precipitation anomalies over the tropical Atlantic and the weakening of the Indian monsoon are always a common feature. The mechanism suggested above could therefore be robust in other models, a detailed comparative analysis of hosing experiments, including sensitivity tests with several models would be of immense benefit to get more insight in this teleconnection.

A possible limitation of the modelling results is a bias in the representation of the Indian monsoon intensity and a bias in the westerly jet position that is too southward in our model (Marti et al., 2010). The impact of variations of the North Atlantic climate is seen across the globe and at different time scales. The validity of this mechanism could also be tested with other models and under different climatic conditions, as a continuity of Swingedouw et al. (2009) who analyze the impact of freshwater hosing experiments for the present, the future, the Holocene, the LGM and the Eemian.

Our data/model comparison is successful in bringing the bigger picture resulting in the Bay of Bengal hydrology cycle changes. However, the fact that not all the low salinity events in the record are correlated with Heinrich events indicates that the complex variability of the Tropics during the last glaciation and its interaction with higher latitudes are not yet fully understood, and some studies suggest that the Tropics and high latitudes interactions should be approached as a more global and coupled feedback in order to explain the abrupt climate changes that happened around the globe (Tierney and Russell, 2007; Seager and Battisti, 2007; Clement and Peterson, 2008). Also, similar detailed analysis of teleconnection mechanisms between North Atlantic climate change and other monsoon systems should be carried as each system could respond in a very different way.

Acknowledgements. All simulations were run at the CEA/CCRT computing centre, which we aknowledge for the computing and storage facilities. We also wish to thank Ramdane Alkama who ran the first fresh water hosing experiment with the IPSL model under glacial conditions.

The publication of this article is financed by CNRS-INSU.

References

Allen, J. R. M., Brandt, U., Brauer, A., Hubberten, H. W., Huntley, B., Keller, J., Kraml, M., Mackensen, A., Mingram, J., Negendank, J. F. W., Nowaczyk, N. R., Oberhansli, H., Watts, W. A., Wulf, S., and Zolitschka, B.: Rapid environmental changes in southern Europe during the last glacial period, Nature, 400, 740–743, 1999. 6271

Altabet, M. A., Higginson, M. J., and Murray, D. W.: The effect of millennial-scale changes in Arabian Sea denitrification on atmospheric CO_2, Nature, 415, 159–162, 2002. 6271, 6277, 6281

An, Z. S., Wu, X. H., Wang, P. X., Wang, S. M., Dong, G. R., Sun, X. J., Zhang, D. E., Lu, Y. C., Zheng, S. H., and Zhao, S. L.: Paleomonsoons of China Over the Last 130,000 Years – Paleomonsoon Variation, Sci. China Ser. B, 34, 1016–1024, 1991. 6276

An, Z. S., Porter, S. C., Zhou, W. J., Lu, Y. C., Donahue, D. J., Head, M. J., Wu, X. H., Ren, J. Z., and Zheng, H. B.: Episode of Strengthened Summer Monsoon Climate of Younger Dryas Age On the Loess Plateau of Central China, Quatern. Res., 39, 45–54, 1993. 6276

Bard, E.: Geochemical and geophysical implications of the radiocarbon calibration, Geochim. Cosmochim. Acta, 62, 2025–2038, 1998. 6275

Barrows, T. and Juggins, S.: Sea-surface temperatures around the Australian margin and Indian Ocean during the Last Glacial Maximum, Quaternary Sci. Rev., 24, 1017–1047, 2005. 6274

Behl, R. J. and Kennett, J. P.: Brief interstadial events in the Santa Barbara basin, NE Pacific, during the past 60 kyr, Nature, 379, 243–246, 1996. 6271

Berger, A. L.: Long-Term Variations Of Daily Insolation And Quaternary Clim. Changes, J. Atmos. Sci., 35, 2362–2367, 1978. 6279

Bond, G., Heinrich, H., Broecker, W., Labeyrie, L., McManus, J., Andrews, J., Huon, S., Jantschik, R., Clasen, S., Simet, C., Tedesco, K., Klas, M., Bonani, G., and Ivy, S.: Evidence for massive discharges of icebergs into the North Atlantic Ocean during the last glacial period, Nature, 360, 245–249, 1992. 6271

Braconnot, P., Otto-Bliesner, B., Harrison, S., Joussaume, S., Peterchmitt, J.-Y., Abe-Ouchi, A., Crucifix, M., Driesschaert, E., Fichefet, Th., Hewitt, C. D., Kageyama, M., Kitoh, A., Laîné, A., Loutre, M.-F., Marti, O., Merkel, U., Ramstein, G., Valdes, P., Weber, S. L., Yu, Y., and Zhao, Y.: Results of PMIP2 coupled simulations of the Mid-Holocene and Last Glacial Maximum – Part 1: experiments and large-scale features, Clim. Past, 3, 261–277, doi:10.5194/cp-3-261-2007, 2007. 6271, 6279, 6280

Broecker, W. S. and Peng, T.-H.: Tracers in the Sea, Lamont-Doherty Geological Observatory, Palisades, NY, 1982. 6275

Broecker, W. S., Bond, G., Klas, M., Clark, E., and McManus, J.: Origin of the northern Atlantic's Heinrich events, Clim. Dynam., 6, 265–273, 1992. 6271

Burns, S. J., Fleitmann, D., Matter, A., Kramers, J., and Al-Subbary, A. A.: Indian Ocean climate and an absolute chronology over Dansgaard/Oeschger events 9 to 13, Science, 301, 1365–1367, 2003. 6271, 6275

Chang, P., Zhang, R., Hazeleger, W., Wen, C., Wan, X. Q., Ji, L., Haarsma, R. J., Breugem, W. P., and Seidel, H.: Oceanic link between abrupt changes in the North Atlantic Ocean and the African monsoon, Nat. Geosci., 1, 444–448, 2008. 6281
Chen, F., Bloemendal, J., Wang, J., Li, J., Oldfield, F., and Ma, H.: High-resolution multi-proxy climate records from Chinese loess: evidence for rapid climatic changes between 70 ka and 10 ka, Paleogeogr. Paleocl., 130, 323–335, 1997. 6276, 6277
Clement, A. C. and Peterson, L. C.: Mechanisms of abrupt climate change of the last glacial period, Rev. Geophys., 46, RG4002, doi:10.1029/2006RG000204, 2008. 6272, 6273, 6287, 6290
COHMAP Members: Clim. Changes of the Last 18,000 Years: Observations and Model Simulations, Science, 241, 1043–1052, 1988. 6276
Cosford, J., Qing, H. R., Yuan, D. X., Zhang, M. L., Holmden, C., Patterson, W., and Hai, C.: Millennial-scale variability in the Asian monsoon: Evidence from oxygen isotope records from stalagmites in Southeastern China, Palaeogeogr. Palaeocl., 266, 3–12, doi:10.1016/j.palaeo.2008.03.029, 2008. 6277
Craig, H. and Gordon, L. I.: Deuterium and oxygen 18 variations in the ocean and the marine atmosphere, Marine Geochemistry, Narragansett Marine Laboratory, University of Rhode Island, 3, 277–374, 1965. 6275
Cullen, J. L.: Microfossil Evidence For Changing Salinity Patterns In the Bay of Bengal Over the Last 20 000 Years, Palaeogeogr. Palaeocl., 35, 315–356, 1981. 6274
Dallenbach, A., Blunier, T., Fluckiger, J., Stauffer, B., Chappellaz, J., and Raynaud, D.: Changes in the atmospheric CH_4 gradient between Greenland and Antarctica during the Last Glacial and the transition to the Holocene, Geophys. Res. Lett., 27, 1005–1008, 2000. 6279
Dansgaard, W., Johnsen, S. J., Clausen, H. B., Dahljensen, D., Gundestrup, N. S., Hammer, C. U., Hvidberg, C. S., Steffensen, J. P., Sveinbjornsdottir, A. E., Jouzel, J., and Bond, G.: Evidence For General Instability Of Past Climate From A 250-Kyr Ice-Core Record, Nature, 364, 218–220, 1993. 6271
Delaygue, G., Bard, E., Rollion, C., Jouzel, J., Stievenard, M., Duplessy, J. C., and Ganssen, G.: Oxygen isotope/salinity relationship in the northern Indian Ocean, J. Geophys. Res.-Oceans, 106, 4565–4574, 2001. 6275, 6276
Ding, Q. H. and Wang, B.: Circtunglobal teleconnection in the Northern Hemisphere summer, J. Climate, 18, 3483–3505, 2005. 6286

Ding, Q. H. and Wang, B.: Intraseasonal teleconnection between the summer Eurasian wave train and the Indian monsoon, J. Climate, 20, 3751–3767, 2007. 6286

Dong, B. W. and Sutton, R. T.: Adjustment of the coupled ocean-atmosphere system to a sudden change in the Thermohaline Circulation, Geophys. Res. Lett., 29, 1728, doi:10.1029/2002GL015229, 2002. 6285

Duplessy, J. C.: Glacial to interglacial contrasts in the northern Indian Ocean, Nature, 295, 494–498, doi:10.1038/295494a0, 1982. 6271, 6274

Duplessy, J. C., Labeyrie, L., Juilletleclerc, A., Maitre, F., Duprat, J., and Sarnthein, M.: Surface Salinity Reconstruction of the North-atlantic Ocean During the Last Glacial Maximum, Oceanol. Acta, 14, 311–324, 1991. 6277

Elliot, M., Labeyrie, L., and Duplessy, J.-C.: Changes in North Atlantic deep-water formation associated with the Dansgaard-Oeschger temperature oscillations (60–10 ka), Quaternary Sci. Rev., 21, 1153–1165, 2002. 6271

Emiliani, D.: Depth habitats of some species of pelagic foraminifera as indicated by oxygen isotope ratios, Am. J. Sci., 252, 149–158, 1954. 6275

EPICA Community Members: One-to-one coupling of glacial climate variability in Greenland and Antarctica, Nature, 444, 195–198, 2006. 6271

Epstein, S. R., Buchsbaum, R., Lowenstam, H. A., and Urey, H. C.: Revised carbonate-water isotopic temperature scale, Geol. Soc. Am. Bull., 64, 1315–1325, 1953. 6274

Fairbanks, R. G., Mortlock, R. A., Chiu, T. C., Cao, L., Kaplan, A., Guilderson, T. P., Fairbanks, T. W., Bloom, A. L., Grootes, P. M., and Nadeau, M. J.: Radiocarbon calibration curve spanning 0 to 50,000 years BP based on paired $^{230}Th/^{234}U/^{238}U$ and ^{14}C dates on pristine corals, Quaternary Sci. Rev., 24, 1781–1796, doi:10.1016/j.quascirev.2005.04.007, 2005. 6275, 6303

Feng, S. and Hu, Q.: How the North Atlantic Multidecadal Oscillation may have influenced the Indian summer monsoon during the past two millennia, Geophys. Res. Lett., 35, L01707, doi:10.1029/2007GL032484, 2008. 6272

Fichefet, T. and Maqueda, M. A. M.: Sensitivity of a global sea ice model to the treatment of ice thermodynamics and dynamics, J. Geophys. Res., 102, 12609–12646, 1997. 6279

Flückiger, J., Dallenbach, A., Blunier, T., Stauffer, B., Stocker, T. F., Raynaud, D., and Barnola, J. M.: Variations in atmospheric N_2O concentration during abrupt climatic changes, Science, 285, 227–230, 1999. 6279

Fontes, J. C., Gasse, F., and Gibert, E.: Holocene environmental changes in Lake Bangong basin (western Tibet), 1. Chronology and stable isotopes of carbonates of a Holocene lacustrine core, Palaeogeogr. Palaeocl., 120, 25–47, 1996. 6276

Gasse, F., Fontes, J. C., VanCampo, E., and Wei, K.: Holocene environmental changes in Bangong Co basin (western Tibet), 4. Discussion and conclusions, Palaeogeogr. Palaeocl., 120, 79–92, 1996. 6276

Goswami, B. N. and Xavier, P. K.: ENSO control on the south Asian monsoon through the length of the rainy season, Geophys. Res. Lett., 32, L18717, doi:10.1029/2005GL023216, 2005. 6272, 6282

Goswami, B. N., Madhusoodanan, M. S., Neema, C. P., and Sengupta, D.: A physical mechanism for North Atlantic SST influence on the Indian summer monsoon, Geophys. Res. Lett., 33, L02706, doi:10.1029/2005GL024803, 2006. 6272, 6285, 6287

Grootes, P. M., Stuiver, M., White, J. W. C., Johnsen, S., and Jouzel, J.: Comparison Of Oxygen-Isotope Records From The Gisp2 And Grip Greenland Ice Cores, Nature, 366, 552–554, 1993. 6271

Guo, Z., Liu, T., Guiot, J., Wu, N., Lu, H., Han, J., Liu, J., and Gu, Z.: High frequency pulses of East Asian monsoon climate in the last two glaciations: Link with the North Atlantic, Clim. Dynam., 12, 701–709, 1996. 6276, 6277

Gupta, A. K., Anderson, D. M., and Overpeck, J. T.: Abrupt changes in the Asian southwest monsoon during the Holocene and their links to the North Atlantic Ocean, Nature, 421, 354–357, 2003. 6281

He, H. Y., Sui, C. H., Jian, M. Q., Wen, Z. P., and Lan, G. D.: The evolution of tropospheric temperature field and its relationship with the onset of Asian summer monsoon, J. Meteorol. Soc. Jpn., 81, 1201–1223, 2003. 6272, 6282

Heinrich, H.: Origin and consequences offset cyclic ice rafting in the northeast Atlantic Ocean during the past 130,000 years, Quatern. Res., 29, 142–152, doi:10.1016/0033-5894(88)90057-9, 1988. 6271

Hourdin, F., Musat, I., Bony, S., Braconnot, P., Codron, F., Dufresne, J. L., Fairhead, L., Filiberti, M. A., Friedlingstein, P., Grandpeix, J. Y., Krinner, G., Levan, P., Li, Z. X., and Lott, F.: The LMDZ4 general circulation model: climate performance and sensitivity to parametrized physics with emphasis on tropical convection, Clim. Dynam., 27, 787–813, 2006. 6278

CPD
8, 6269–6308, 2012

Indian monsoon and North Atlantic abrupt climate change

C. Marzin et al.

Hughen, K., Lehman, S., Southon, J., Overpeck, J., Marchal, O., Herring, C., and Turnbull, J.: ^{14}C activity and global carbon cycle changes over the past 50,000 years, Science, 303, 202–207, 2004. 6275

Hutson, W.: The Agulhas Current during the Late Pleistocene: Analysis of modern faunal analogs, Science, 207, 64–66, 1979. 6274

Jin, L., Chen, F., Ganopolski, A., and Claussen, M.: Response of East Asian climate to Dansgaard/Oeschger and Heinrich events in a coupled model of intermediate complexity, J. Geophys. Res.-Atmos., 112, D06117, doi:10.1029/2006JD007316, 2007. 6272

Kageyama, M., Mignot, J., Swingedouw, D., Marzin, C., Alkama, R., and Marti, O.: Glacial climate sensitivity to different states of the Atlantic Meridional Overturning Circulation: results from the IPSL model, Clim. Past, 5, 551–570, doi:10.5194/cp-5-551-2009, 2009. 6273, 6279, 6281, 6282, 6286

Kageyama, M., Paul, A., Roche, D. M., and Meerbeeck, C. J. V.: Modelling glacial climatic millennial-scale variability related to changes in the Atlantic meridional overturning circulation: a review, Quaternary Sci. Rev., 29, 2931–2956, doi:10.1016/j.quascirev.2010.05.029, 2010. 6273

Khare, N.: Climatically sensitive 'Arctic': Another scientific frontier for India, Current Sci., 94, 176–178, 2008. 6272

Krinner, G., Viovy, N., de Noblet-Ducoudre, N., Ogee, J., Polcher, J., Friedlingstein, P., Ciais, P., Sitch, S., and Prentice, I. C.: A dynamic global vegetation model for studies of the coupled atmosphere-biosphere system, Global Biogeochem. Cy., 19, GB1015, doi:10.1029/2003GB002199, 2005. 6278

Kucharski, F., Bracco, A., Yoo, J. H., and Molteni, F.: Atlantic forced component of the Indian monsoon interannual variability, Geophys. Res. Lett., 35, L04706, doi:10.1029/2007GL033037, 2008. 6286

Kucharski, F., Bracco, A., Yoo, J. H., Tompkins, A. M., Feudale, L., Ruti, P., and Dell'Aquila, A.: A Gill-Matsuno-type mechanism explains the tropical Atlantic influence on African and Indian monsoon rainfall, Q. J. Roy. Meteorol. Soc., 135, 569–579, 2009. 6286

Kudrass, H. R., Hofmann, A., Doose, H., Emeis, K., and Erlenkeuser, H.: Modulation and amplification of climatic changes in the Northern Hemisphere by the Indian summer monsoon during the past 80 k.y., Geology, 29, 63–66, 2001. 6274

Laj, C., Mazaud, A., and Duplessy, J. C.: Geomagnetic intensity and ^{14}C abundance in the atmosphere and ocean during the past 50 kyr, Geophys. Res. Lett., 23, 2045–2048, 1996. 6275

Li, Y. F. and Harrison, S. P.: Simulations of the impact of orbital forcing and ocean on the Asian summer monsoon during the Holocene, Global Planet. Change, 60, 505–522, 2008. 6272

Losada, T., Rodriguez-Fonseca, B., Polo, I., Janicot, S., Gervois, S., Chauvin, F., and Ruti, P.: Tropical response to the Atlantic Equatorial mode: AGCM multimodel approach, Clim. Dynam., 35, 45–52, 2010. 6286

Lu, R. Y. and Dong, B. W.: Response of the Asian Summer Monsoon to Weakening of Atlantic Thermohaline Circulation, Adv. Atmos. Sci., 25, 723–736, 2008. 6272, 6285

Lu, R. Y., Dong, B. W., and Ding, H.: Impact of the Atlantic multidecadal oscillation on the Asian summer monsoon, Geophys. Res. Lett., 33, L24701, doi:10.1029/2006GL027655, 2006. 6272

Madec, G., Delecluse, P., Imbard, M., and Levy, C.: OPA version 8.1 ocean general circulation model reference manual, LODYC/IPSL, Paris, France, p. 11, 1998. 6278

Marti, O., Braconnot, P., Dufresne, J.-L., Bellier, J., Benshila, R., Bony, S., Brockmann, P., Cadule, P., Caubel, A., Codron, F., Denvil, S., Fairhead, L., Fichefet, T., Foujols, M. A., Friedlingstein, P., Goosse, H., Grandpeix, J. Y., Guilyardi, E., Hourdin, F., Idelkadi, A., Kageyama, M., Krinner, G., Levy, C., Madec, G., Musat, I., Swingedouw, D., and Talandier, C.: Key features of the IPSL ocean atmosphere model and its sensitivity to atmospheric resolution, Clim. Dynam., 34, 1–26, doi:10.1007/s00382-009-0640-6, 2010. 6278, 6279

Marzin, C. and Braconnot, P.: Variations of Indian and African monsoons induced by insolation changes at 6 and 9.5 kyr BP, Clim. Dynam., 33, 215–231, 2009. 6279

McManus, J., Oppo, D., and Cullen, J.: A 0.5-million-year record of millennial-scale climate variability in the North Atlantic, Science, 283, 971–975, doi:10.1126/science.283.5404.971, 1999. 6271

McManus, J. F., Francois, R., Gherardi, J.-M., Keigwin, K., and Brown-Leger, S.: Collapse and rapid resumption of Atlantic meridional circulation linked to deglacial climate changes, Nature, 428, 834–837, 2004. 6271

Meese, D. A., Gow, A. J., Alley, R. B., Zielinski, G. A., Grootes, P. M., Ram, M., Taylor, K. C., Mayewski, P. A., and Bolzan, J. F.: The Greenland Ice Sheet Project 2 depth-age scale: Methods and results, J. Geophys. Res.-Oceans, 102, 26411–26423, 1997. 6271

Merkel, U., Prange, M., and Schulz, M.: ENSO variability and teleconnections during glacial climates, Quaternary Sci. Rev., 29, 86–100, doi:10.1016/j.quascirev.2009.11.006, 2010. 6273

Monnin, E., Indermuhle, A., Dallenbach, A., Fluckiger, J., Stauffer, B., Stocker, T. F., Raynaud, D., and Barnola, J. M.: Atmospheric CO_2 concentrations over the last glacial termination, Science, 291, 112–114, 2001. 6279

Ngo-Duc, T., Laval, K., Polcher, J., Lombard, A., and Cazenave, A.: Effects of land water storage on global mean sea level over the past half century, Geophys. Res. Lett., 32, L09704, doi:10.1029/2005GL022719, 2005. 6278

Otto-Bliesner, B. L. and Brady, E. C.: The sensitivity of the climate response to the magnitude and location of freshwater forcing: last glacial maximum experiments, Quaternary Sci. Rev., 29, 56–73, doi:10.1016/j.quascirev.2009.07.004, 2010. 6273

Overpeck, J. T., Webb, T., and Prentice, I. C.: Quantitative Interpretation of Fossil Pollen Spectra – Dissimilarity Coefficients and the Method of Modern Analogs, Quatern. Res., 23, 87–108, 1985. 6274

Peltier, W. R.: Global glacial isostasy and the surface of the ice-age earth: The ice-5G (VM2) model and grace, Annu. Rev. Earth Planet. Sci., 32, 111–149, 2004. 6279

Porter, S. C. and An, Z. S.: Correlation Between Climate Events In The North-Atlantic And China During Last Glaciation, Nature, 375, 305–308, 1995. 6276, 6277

Prell, W. L., Hutson, W. H., Williams, D. F., Be, A. W. H., Geitzenauer, K., and Molfino, B.: Surface Circulation of the Indian-ocean During the Last Glacial Maximum, Approximately 18,000 Yr Bp, Quatern. Res., 14, 309–336, 1980. 6271

Prentice, I. C.: Multidimensional-scaling As A Research Tool In Quaternary Palynology – A Review of Theory and Methods, Rev. Palaeobot. Palynol., 31, 71–104, 1980. 6274

Rashid, H., Flower, B. P., Poore, R. Z., and Quinn, T. M.: A similar to 25 ka Indian Ocean monsoon variability record from the Andaman Sea, Quaternary Sci. Rev., 26, 2586–2597, 2007. 6274, 6276

Rostek, F., Ruhland, G., Bassinot, F. C., Muller, P. J., Labeyrie, L. D., Lancelot, Y., and Bard, E.: Reconstructing Sea-surface Temperature and Salinity Using Delta-o-18 and Alkenone Records, Nature, 364, 319–321, 1993. 6276

Rousseau, D. D. and Kukla, G.: Abrupt retreat of summer monsoon at the S1/L1 boundary in China, Global Planet. Change, 26, 189–198, 2000. 6271

Schulz, H., von Rad, U., and Erlenkeuser, H.: Correlation between Arabian Sea and Greenland climate oscillations of the past 110,000 years, Nature, 393, 54–57, 1998. 6281

Seager, R. and Battisti, D. S.: The General Circulation of the Atmosphere, chap. Challenges to our understanding of the general circulation: Abrupt climate change, Princeton University Press, 331–371, 2007. 6290

Shackleton, N. J.: Attainment of isotopic equilibrium between ocean water and benthonic foraminifera genus Uvigerina: Isotopic changes in the ocean during the last glacial, Colloq. Int. C.N.R.S., 219, 203–209, 1974. 6274

Sirocko, F., Sarnthein, M., Lange, H., and Erlenkeuser, H.: Atmospheric Summer Circulation and Coastal Upwelling In the Arabian Sea During the Holocene and the Last Glaciation, Quatern. Res., 36, 72–93, 1991. 6276, 6278

Stocker, T. F. and Johnsen, S. J.: A minimum thermodynamic model for the bipolar seesaw, Paleoceanography, 18, 1087, doi:10.1029/2003PA000920, 2003. 6271

Stouffer, R. J., Yin, J., Gregory, J. M., Dixon, K. W., Spelman, M. J., Hurlin, W., Weaver, A. J., Eby, M., Flato, G. M., Hasumi, H., Hu, A., Jungclaus, J. H., Kamenkovich, I. V., Levermann, A., Montoya, M., Murakami, S., Nawrath, S., Oka, A., Peltier, W. R., Robitaille, D. Y., Sokolov, A., Vettoretti, G., and Weber, S. L.: Investigating the causes of the response of the thermohaline circulation to past and future climate changes, J. Climate, 19, 1365–1387, 2006. 6281

Stuiver, M. and Reimer, P. J.: Extended ^{14}C Data-base and Revised Calib 3.0 ^{14}C Age Calibration Program, Radiocarbon, 35, 215–230, 1993. 6275, 6303

Stuiver, M., Reimer, P. J., and Braziunas, T. F.: High-precision radiocarbon age calibration for terrestrial and marine samples, Radiocarbon, 40, 1127–1151, 1998. 6275, 6303

Swingedouw, D., Mignot, J., Braconnot, P., Mosquet, E., Kageyama, M., and Alkama, R.: Impact of Freshwater Release in the North Atlantic under Different Climate Conditions in an OAGCM, J. Climate, 22, 6377–6403, 2009. 6281, 6286, 6289

Thouveny, N., Debeaulieu, J. L., Bonifay, E., Creer, K. M., Guiot, J., Icole, M., Johnsen, S., Jouzel, J., Reille, M., Williams, T., and Williamson, D.: Climate Variations In Europe Over The Past 140-Kyr Deduced From Rock Magnetism, Nature, 371, 503–506, 1994. 6271

Tierney, J. E. and Russell, J. M.: Abrupt climate change in southeast tropical Africa influenced by Indian monsoon variability and ITCZ migration, Geophys. Res. Lett., 34, L15709, doi:10.1029/2007GL029508, 2007. 6290

Timmermann, A., Okumura, Y., An, S. I., Clement, A., Dong, B., Guilyardi, E., Hu, A., Jungclaus, J. H., Renold, M., Stocker, T. F., Stouffer, R. J., Sutton, R., Xie, S. P., and Yin, J.: The influence of a weakening of the Atlantic meridional overturning circulation on ENSO, J. Climate, 20, 4899–4919, 2007. 6281

Valcke, S.: OASIS3 user guide (prism_2-5), PRISM support initiative 3, http://www.prism.enes.org/Publications/Reports/oasis3_UserGuide_T3.pdf, last access: December 2012, 68 pp., 2006. 6279

van der Plicht, J., Beck, J. W., Bard, E., Baillie, M. G. L., Blackwell, P. G., Buck, C. E., Friedrich, M., Guilderson, T. P., Hughen, K. A., Kromer, B., McCormac, F. G., Ramsey, C. B., Reimer, P. J., Reimer, R. W., Remmele, S., Richards, D. A., Southon, J. R., Stuiver, M., and Weyhenmeyer, C. E.: NotCal04 – Comparison/calibration ^{14}C records 26–50 cal kyr BP, Radiocarbon, 46, 1225–1238, 2004. 6275

VanCampo, E. and Gasse, F.: Pollen-inferred and Diatom-inferred Climatic and Hydrological Changes In Sumxi Co Basin (western Tibet) Since 13,000 Yr Bp, Quatern. Res., 39, 300–313, 1993. 6276

VanCampo, E., Cour, P., and Hang, S. X.: Holocene environmental changes in Bangong Co basin (western Tibet), 2. The pollen record, Palaeogeogr. Palaeocl., 120, 49–63, 1996. 6276

Varkey, M. J., Murty, V. S. N., and Suryanarayana, A.: Oceanography and Marine Biology: an Annual Review, chap. Physical oceanography of the Bay of Bengal and Andaman Sea, UCL Press, 1–70, 1996. 6282

Vellinga, M. and Wood, R. A.: Global climatic impacts of a collapse of the Atlantic thermohaline circulation, Climatic Change, 54, 251–267, 2002. 6272

Voelker, A., Sarnthein, M., Grootes, P., Erlenkeuser, H., Laj, C., Mazaud, A., Nadeau, M.-J., and Schleicher, M.: Correlation of marine ^{14}C ages from the Nordic Sea with the GISP2 isotope record: Implications for ^{14}C calibration beyond 25 ka BP, Radiocarbon, 40, 517–534, 1998. 6275

Waelbroeck, C., Labeyrie, L., Michel, E., Duplessy, J. C., McManus, J. F., Lambeck, K., Balbon, E., and Labracherie, M.: Sea-level and deep water temperature changes derived from benthic foraminifera isotopic records, Quaternary Sci. Rev., 21, 295–305, 2002. 6275

Wang, Y. J., Cheng, H., Edwards, R. L., An, Z. S., Wu, J. Y., Shen, C. C., and Dorale, J. A.: A high-resolution absolute-dated Late Pleistocene monsoon record from Hulu Cave, China, Science, 294, 2345–2348, 2001. 6271, 6275, 6277

Wu, R. G. and Kirtman, B. P.: Observed relationship of spring and summer East Asian rainfall with winter and spring Eurasian snow, J. Climate, 20, 1285–1304, 2007. 6281

Xavier, P. K., Marzin, C., and Goswami, B. N.: An objective definition of the Indian summer monsoon season and a new perspective on the ENSO-monsoon relationship, Q. J. Roy. Meteorol. Soc., 133, 749–764, 2007. 6285

Xiao, J. L., Porter, S. C., An, Z. S., Kumai, H., and Yoshikawa, S.: Grain-size of Quartz As An Indicator of Winter Monsoon Strength On the Loess Plateau of Central China During the Last 130,000-yr, Quatern. Res., 43, 22–29, 1995. 6276, 6277

Xiao, J. L., An, Z. S., Liu, T. S., Inouchi, Y., Kumai, H., Yoshikawa, S., and Kondo, Y.: East Asian monsoon variation during the last 130,000 Years: evidence from the Loess Plateau of central China and Lake Biwa of Japan, Quaternary Sci. Rev., 18, 147–157, 1999. 6271

Yanase, W. and Abe-Ouchi, A.: The LGM surface climate and atmospheric circulation over East Asia and the North Pacific in the PMIP2 coupled model simulations, Clim. Past, 3, 439–451, doi:10.5194/cp-3-439-2007, 2007. 6270

Zhang, R. and Delworth, T. L.: Simulated tropical response to a substantial weakening of the Atlantic thermohaline circulation, J. Climate, 18, 1853–1860, 2005. 6272, 6285

Zhang, R. and Delworth, T. L.: Impact of Atlantic multidecadal oscillations on India/Sahel rainfall and Atlantic hurricanes, Geophys. Res. Lett., 33, L17712, doi:10.1029/2006GL026267, 2006. 6272

Zonneveld, K. A. F., Ganssen, G., Troelstra, S., Versteegh, G. J. M., and Visscher, H.: Mechanisms forcing abrupt fluctuations of the Indian Ocean summer monsoon during the last deglaciation, Quaternary Sci. Rev., 16, 187–201, 1997. 6276, 6278

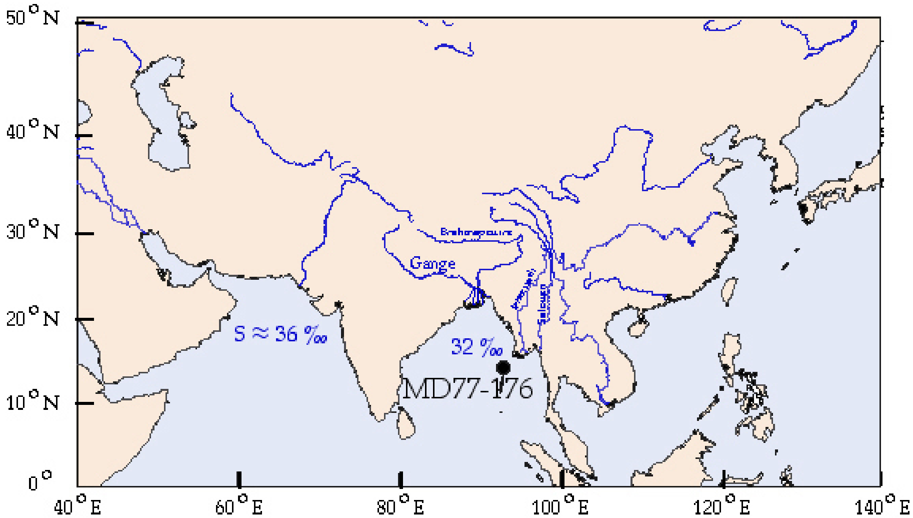

Fig. 1. Location map of the sediment core MD77-176 in the Bay of Bengal: 14°31′ N; 93°08′ E; 1375 m water depth.

CPD
8, 6269–6308, 2012

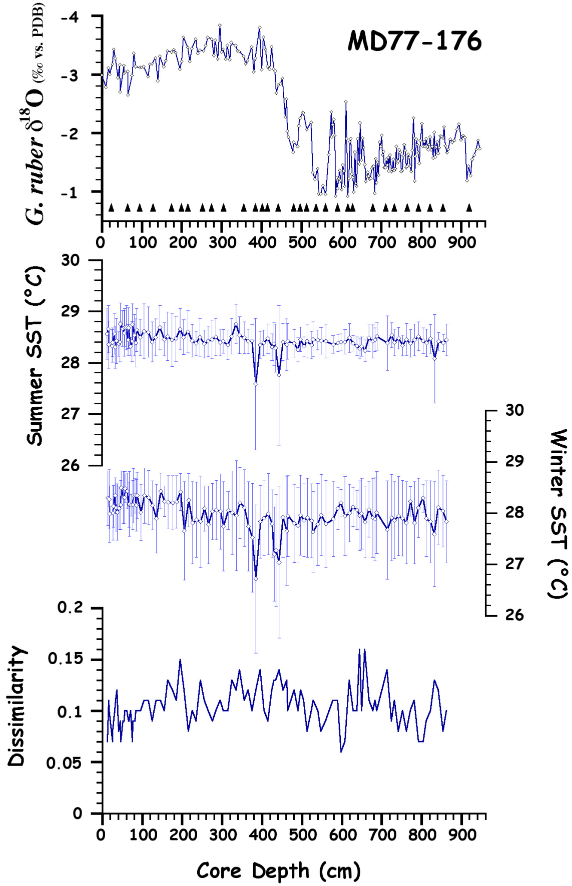

Fig. 2. Depth-age plots for core MD77-176. From top to bottom: $\delta^{18}O$ of *G. ruber*, reconstructions of summer sea surface temperatures (SST) and winter SST with error bars and dissimilarity coefficients between fossil assemblages and the modern analogues.

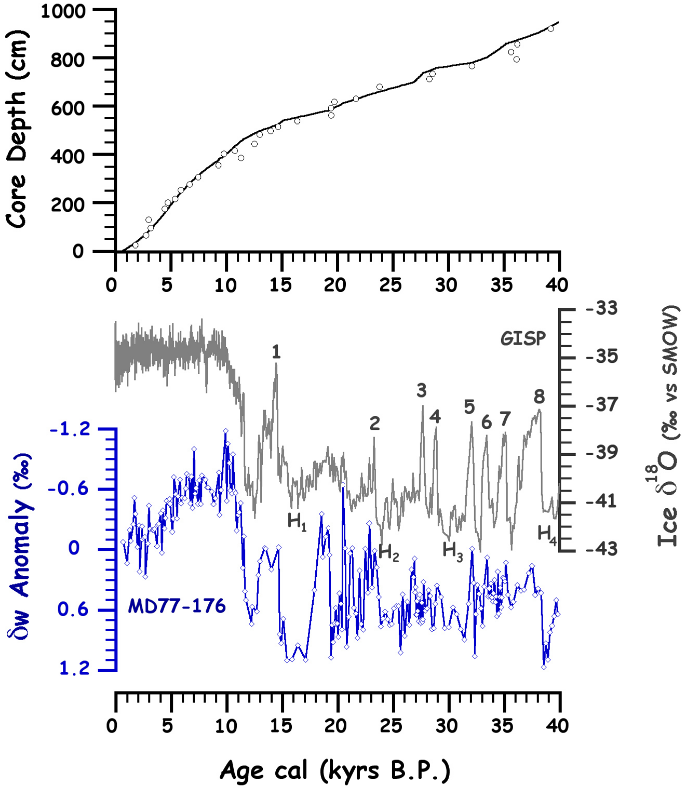

Fig. 3. From top to bottom: MD77-176 core depth versus age (circles represent ^{14}C ages converted into calendar ages using the Calib 4.1 program (Stuiver and Reimer, 1993; Stuiver et al., 1998) after 20 ky ^{14}C BP and Fairbanks et al. (2005) calibration before. Line represents the age model developed assuming that changes in the Northern Andaman Sea and GISP2 are in phase and synchronous), Greenland ice core record GISP2 ice $\delta^{18}O$ versus age and MD77-176 core δ_w anomaly versus age.

CPD
8, 6269–6308, 2012

Indian monsoon and North Atlantic abrupt climate change

C. Marzin et al.

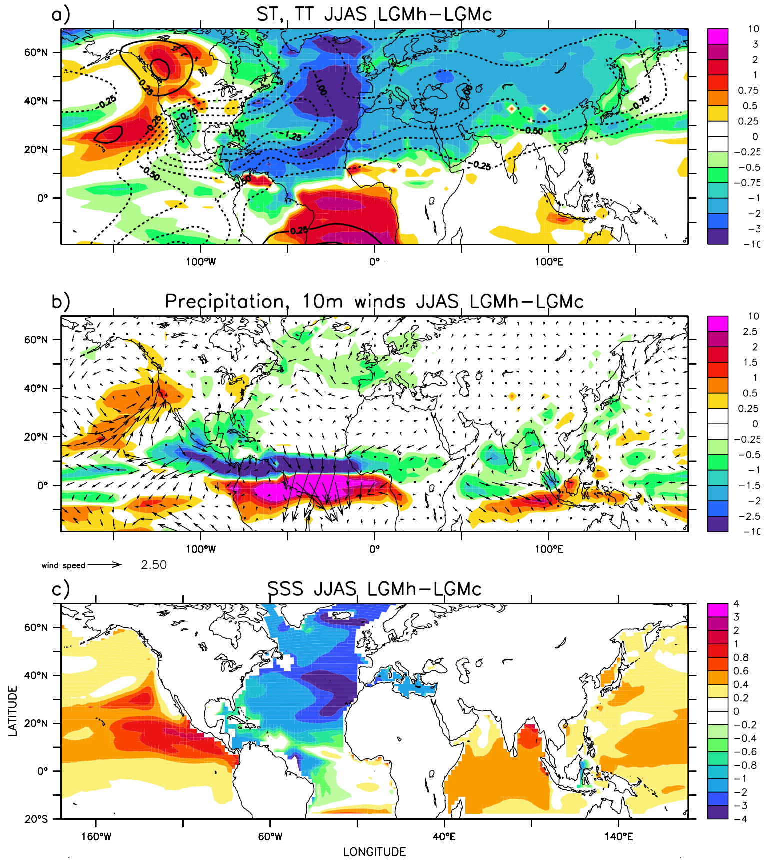

Fig. 4. Differences between LGMh and LGMc (hosing minus control experiment) of **(a)** JJAS (June to September mean) surface temperature (ST, shaded) and tropospheric temperature averaged from 200 to 500 hPa (TT, contours), **(b)** precipitation and 10 m winds, **(c)** sea surface salinity (SSS).

CPD
8, 6269–6308, 2012

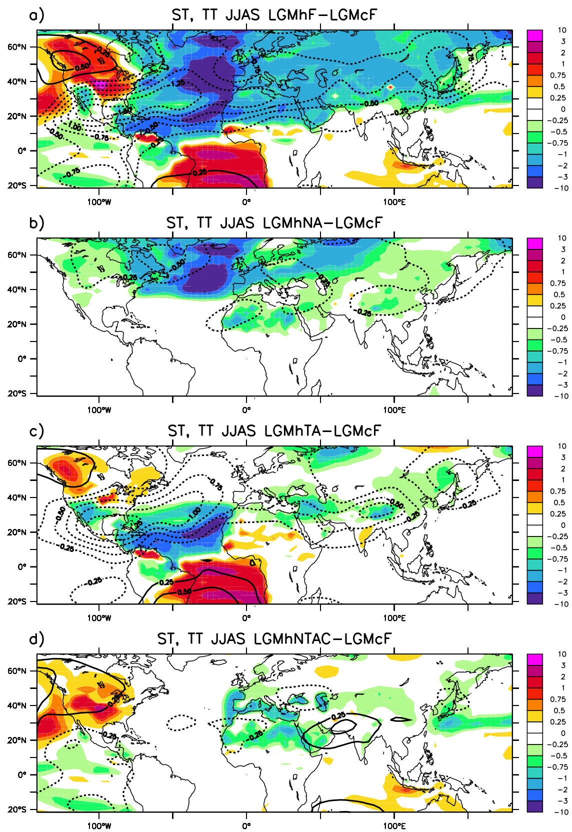

Fig. 5. Differences of JJAS surface temperature (ST, shaded) and tropospheric temperature averaged from 200 to 500 hPa (TT, contours) between **(a)** LGMhF and LGMcF (hosing minus control experiment), **(b)** LGMhNA and LGMcF (North Atlantic minus control experiment), **(c)** LGMhTA and LGMcF (tropical Atlantic minus control experiment), **(d)** LGMhNTAC and LGMcF (complementary minus control experiment).

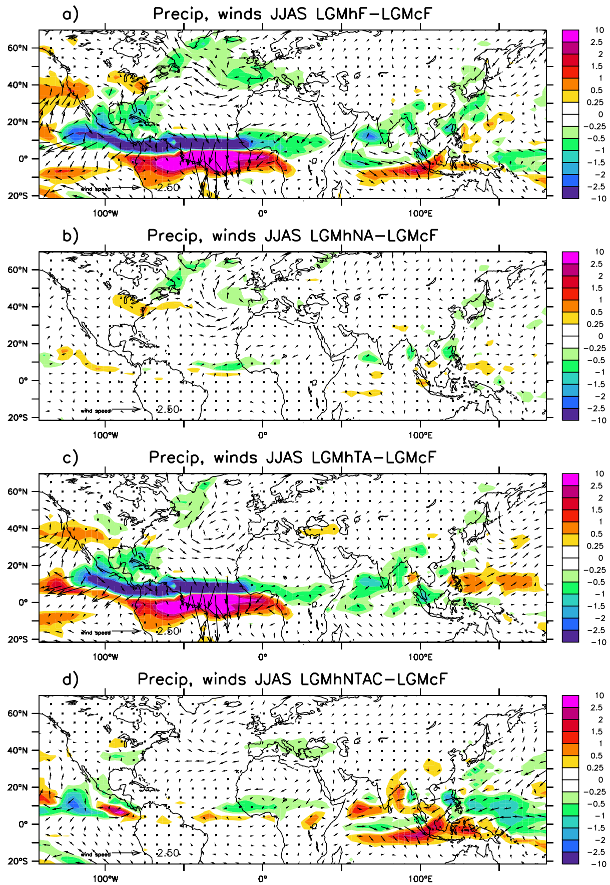

Fig. 6. Differences of JJAS precipitation and 10 m winds between **(a)** LGMhF and LGMcF, **(b)** LGMhNA and LGMcF, **(c)** LGMhTA and LGMcF, **(d)** LGMhNTAC and LGMcF.

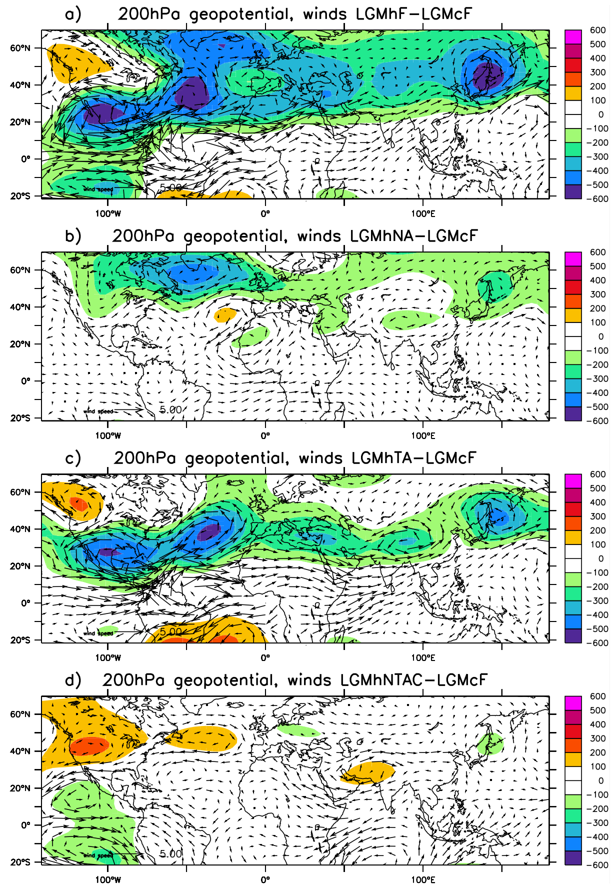

Fig. 7. Differences of JJAS 200 hPa geopotential and winds between **(a)** LGMhF and LGMcF, **(b)** LGMhNA and LGMcF, **(c)** LGMhTA and LGMcF, **(d)** LGMhNTAC and LGMcF.

CPD
8, 6269–6308, 2012

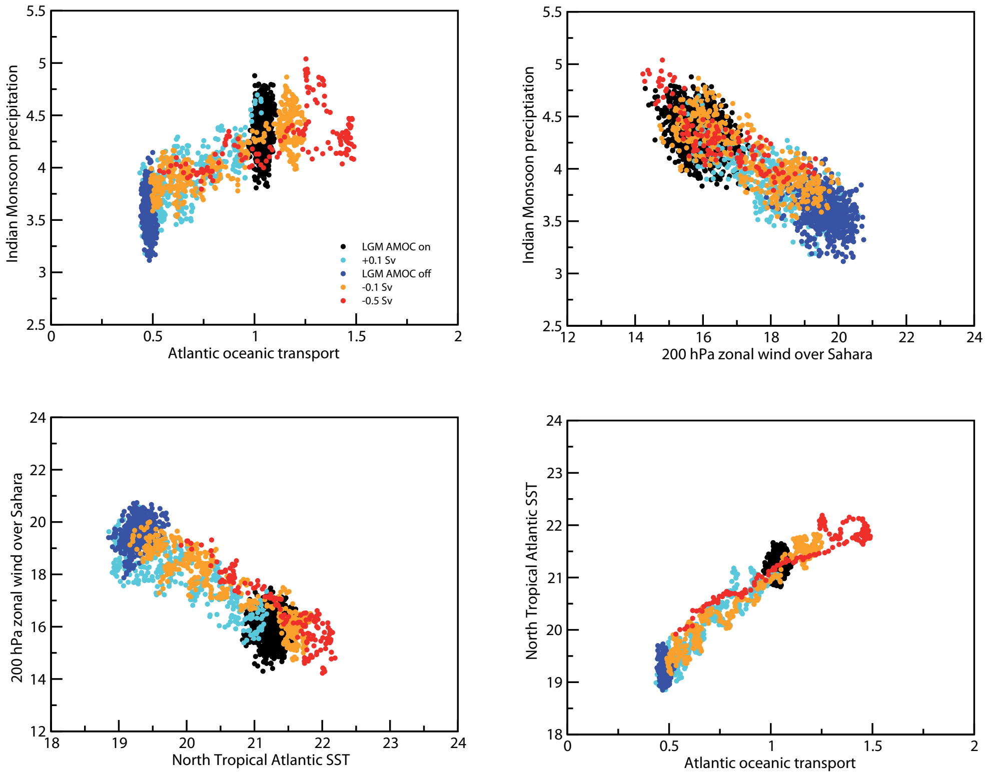

Fig. 8. Yearly JJAS values of Indian monsoon precipitation (mm day^{-1}) over the region (60–80° E, 5–15° N) vs. Atlantic oceanic transport (Sv) (top left panel), Indian monsoon precipitation (mm day^{-1}) vs. 200 hPa zonal wind (m s^{-1}) over the Sahara (15° W–45° E, 10–30° N) (top right panel), 200 hPa zonal wind over the Sahara vs. North tropical Atlantic SST (°C) over the region (45–15° W, 10–30° N) (bottom left panel) and North tropical Atlantic SST vs. Atlantic oceanic transport (bottom right panel).